



**The Abdus Salam
International Centre for Theoretical Physics**



2152-17

**Joint ICTP-IAEA Course on Natural Circulation Phenomena and
Passive Safety Systems in Advanced Water Cooled Reactors**

17 - 21 May 2010

Passive Safety System Design & Certification Testing in APEX and NuScale

Jose N. Reyes Jr.
Oregon State University
USA

AP600 AND AP1000 PASSIVE SAFETY SYSTEM DESIGN AND TESTING IN APEX

José N. Reyes, Jr*

Oregon State University, USA

Abstract

This lecture describes the integral operation of the AP600/AP1000 passive safety systems. It presents methods to calculate and scale injection flow rates for gravity drain tanks and pressurized tanks and a method to estimate depressurization flow rates for an ADS system.

1. INTRODUCTION

The application of passive safety systems in new nuclear power plants is a potential means of achieving simplification and improving economics. The use of passive systems is not entirely new, and is not unique to any particular line of new reactor designs. But an increased reliance on this approach, making safety functions less dependent on active components like pumps and diesel generators, is potentially an important means to achieve reduced costs for future nuclear power plants. Many new reactor designs that are under development incorporate passive systems based on natural circulation.

The purpose of this lecture is to introduce the passive safety systems used in the Westinghouse *Advanced Passive 600* MWe (AP600) and *Advanced Passive 1000* MWe (AP1000) nuclear plant designs and to provide some simple modeling and scaling techniques for these systems.

1.1. Definition of passive safety systems

What is meant by a passive safety system? A passive safety system provides cooling to the nuclear core using processes such as, natural convection heat transfer, vapor condensation, liquid evaporation, pressure driven coolant injection, or gravity driven coolant injection. It does not rely on external mechanical and/or electrical power, signals or forces such as electric pumps. A useful list of terminology related to passive safety is found in IAEA-TECDOC-626 [1] It is important to note that passive safety systems can provide an equal or greater degree of safety as active safety systems used in conventional plants. For example, to obtain final design approval in the U.S., a passively safe nuclear plant must demonstrate that under worst-case accident conditions the plant can be passively cooled without external power or operator actions for a minimum of 3 days [2].

2. DESCRIPTION OF AP600/AP1000 DESIGN AND PASSIVE SAFETY SYSTEMS

The AP600 and AP1000 are pressurized light water nuclear reactors designed to produce thermal powers of 1933 MW and 3400 MW, respectively [3]. Figure 1 shows the overall layout of the plant. Figure 2 is a schematic that illustrates the primary system components. The primary loop consists of the reactor vessel, which contains the nuclear fuel assemblies; two hot legs, which connect the reactor vessel to the steam generators; two steam generators; a pressurizer; four canned motor pumps; and four cold legs.

Normal full power operation is straightforward. Heat is generated in the reactor fuel. This heat is transported by forced convection to the water. Since the entire system operates at 15.5 MPa (2250 psia), bulk boiling of the water does not occur. The heated water is transported through the hot legs to the U-tubes inside the steam generators. The energy of the primary coolant inside the tubes is transferred to the water on the secondary side by forced convection inside the tubes, conduction through the tube walls and boiling on the outside surface of the U-tubes. The cooled water leaving the steam generator is pumped by four canned motor pumps, through four cold legs, back into the reactor

* Henry and Janice Schuette Endowed Chair Professor of Nuclear Engineering Department of Nuclear Engineering and Radiation Health Physics, Oregon State University, Corvallis, Oregon, USA, 97331.

vessel where the heating cycle is repeated. Primary system pressure is maintained constant by the pressurizer.

2.1. AP600/AP1000 passive safety systems

With respect to thermal hydraulic phenomena, normal full-power operation is typical of most pressurized water reactor (PWR) systems. A key feature of the AP600 and AP1000 designs is that it uses core decay heat to drive the core cooling process. In fact, the AP600/AP1000 designs use core decay heat to drive the following six natural circulation processes:

- Primary System Natural Circulation (2x4 Loop),
- PRHR Loop Circulation (1 Loop),
- CMT Loop Circulation (2 loops),
- Lower Containment Sump Recirculation (2 loops),
- Containment Internal Circulation (Steam),
- Containment External Circulation (Air).

Figure 3 presents a simple schematic that describes the connections of the primary system passive safety systems.

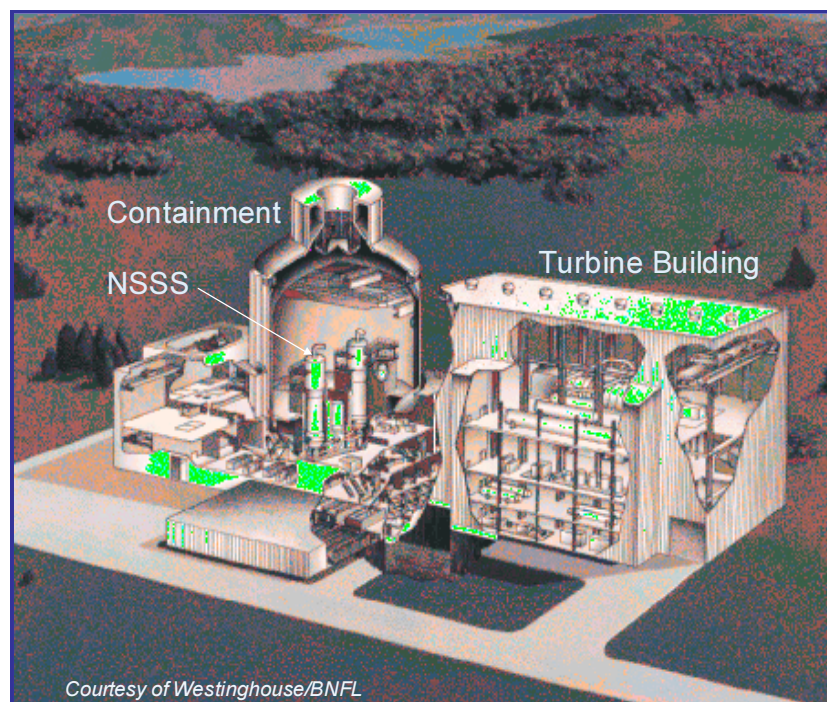


FIG. 1. General layout of the AP600 and AP1000 plants.

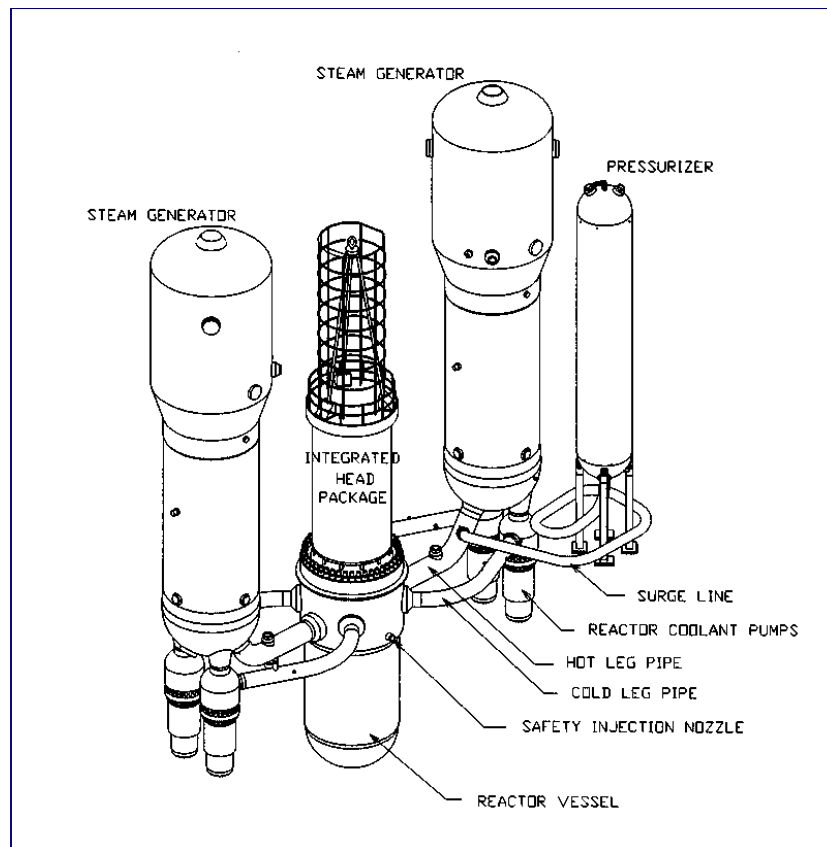


FIG. 2. Schematic of primary loop of the AP600 and AP1000 plants.

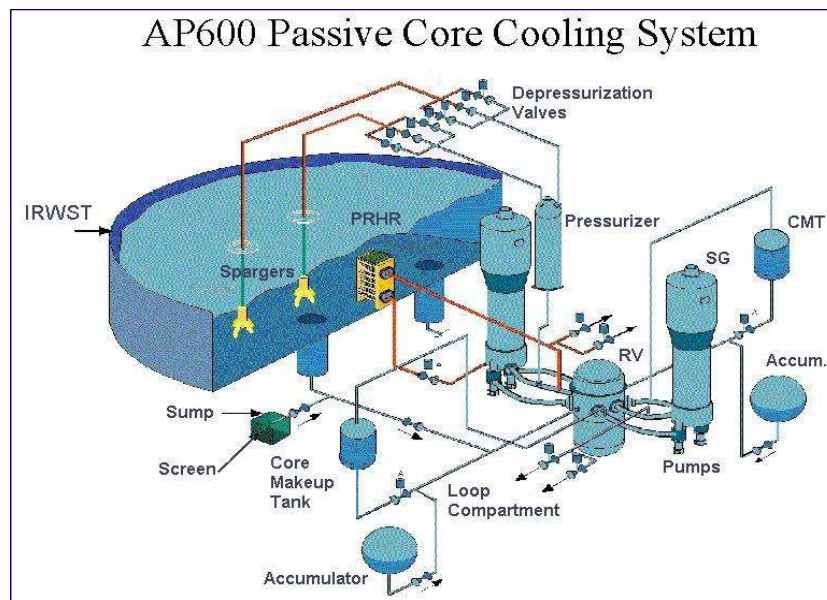


FIG. 3. Passive safety systems used in the AP600/AP1000 designs.

The AP600/AP1000 passive safety systems consist of:

- A Passive Residual Heat Removal (PRHR) System
- Two Core Make-up Tanks (CMTs)
- A Four Stage Automatic Depressurization System (ADS)
- Two Accumulator Tanks (ACC)
- An In-containment Refueling Water Storage Tank, (IRWST)
- A Lower Containment Sump (CS)
- Passive Containment Cooling System (PCCS)

Passive Residual Heat Removal (PRHR) System: The passive residual heat removal (PRHR) consists of a C-Tube type heat exchanger that resides in the water-filled In-containment Refueling Water Storage Tank (IRWST) as shown in the schematic given in Figure 4. The PRHR provides primary coolant heat removal via a natural circulation loop. Hot water rises through the PRHR inlet line attached to one of the hot legs. The hot water enters the tubesheet in the top header of the PRHR heat exchanger at full system pressure and temperature. The IRWST is filled with cold borated water and is open to containment. Heat removal from the PRHR heat exchanger occurs by boiling on the outside surface of the tubes. The cold primary coolant returns to the primary loop via the PRHR outlet line that is connected to the steam generator lower head.

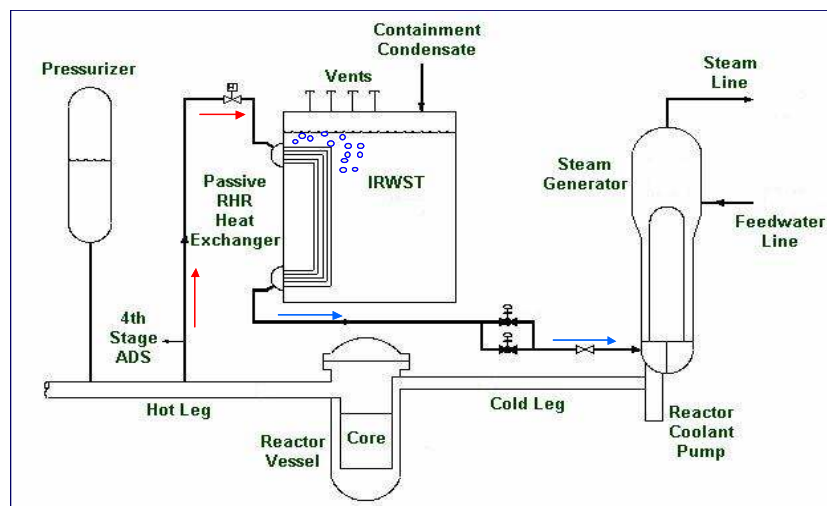


FIG. 4. Passive residual heat removal (PRHR) system.

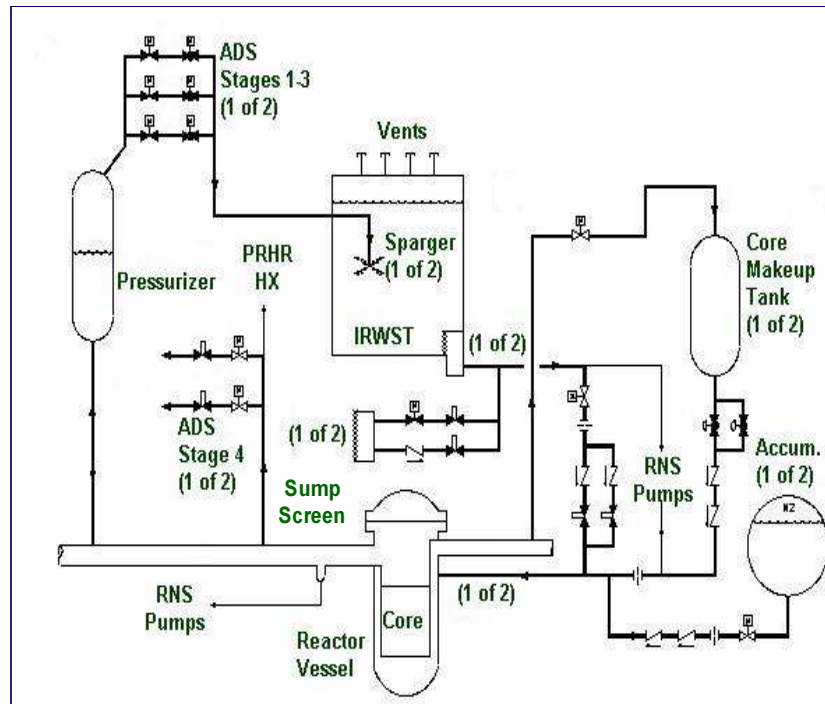


FIG. 5. Passive safety injection and sump recirculation.

Core Make-up Tank (CMT): The Core Make-up Tanks effectively replace the high-pressure safety injection systems in conventional PWRs. Each CMT consists of a large volume stainless steel tank with an inlet line that connects one of the cold legs to the top of the CMT and an outlet line that connects the bottom of the CMT to the Direct Vessel Injection (DVI) line. The DVI line is connected to the reactor vessel downcomer. Each CMT is filled with cold borated water. The CMT inlet valve is normally open and hence the CMT is normally at primary system pressure. The CMT outlet valve is normally closed, preventing natural circulation during normal operation. When the outlet valve is open, a natural circulation path is established. Cold borated water flows to the reactor vessel and hot primary fluid flows upward into the top of the CMT.

Automatic Depressurization System (ADS): The Automatic Depressurization System consists of four stages of valves that provide for the controlled reduction of primary system pressure. The first three stages consist of two trains of valves connected to the top of the pressurizer. The first stage opens on CMT liquid level. ADS stages two and three open shortly thereafter on timers. The ADS 1-3 valves discharge primary system steam into a sparger line that vents into the IRWST. The steam is condensed by direct contact with the highly subcooled water in the IRWST. The fourth stage of the ADS consists of two large valves attached to ADS lines on each hot leg. The ADS-4 valves open on low CMT liquid level and effectively bring primary side pressure down to containment conditions. The ADS-4 valves vent directly into the containment building.

Accumulators (ACC): The accumulators are similar to those found in conventional PWRs. They are large spherical tanks approximately three-quarters filled with cold borated water and pre-pressurized with nitrogen. The accumulator outlet line is connected to the DVI line. A pair of check valves prevents injection flow during normal operating conditions. When system pressure drops below the accumulator pressure (plus the check valve cracking pressure), the check valves open allowing coolant injection to the reactor downcomer via the DVI line.

In-containment Refuelling Water Storage Tank (IRWST): The In-containment Refuelling Water Storage Tank is a very large concrete pool filled with cold borated water. It serves as the heat sink for the PRHR heat exchanger and a source of water for IRWST injection. The IRWST has two injection lines connected to the reactor vessel DVI lines. These flow paths are normally isolated by two check valves in series. When the primary pressure drops below the head pressure of the water in the IRWST,

the flow path is established through the DVI into the reactor vessel downcomer. The IRWST water is sufficient to flood the lower containment compartments to a level above the reactor vessel head and below the outlet of the ADS-4 lines.

Containment Sump Recirculation: After the lower containment sump and the IRWST liquid levels are equalized, the sump valves are opened to establish a natural circulation path. Primary coolant is boiled in the reactor core by decay heat. This low-density mixture flows upward through the core and steam and liquid is vented out of the ADS-4 lines into containment. Cooler water from the containment sump is drawn in through the sump screens into the sump lines that connect to the DVI lines.

Containment and Passive Containment Cooling System (PCCS): Figure 6 presents a schematic of the AP600/AP1000 containment. It consists of a large steel vessel that houses the Nuclear Steam Supply System (NSSS) and all of the passive safety injection systems. The steel containment vessel resides inside of a concrete structure with ducts that allows cool outside air to come in contact with the outside surface of the containment vessel. When steam is vented into containment via a primary system break or ADS-4 valve actuation, it rises to the containment dome where it is condensed into liquid. The energy of the steam is transferred to the air on the outside of containment via conduction through the containment wall and natural convection to the air. As the air is heated, it rises through the ducts creating a natural circulation flow path that draws cool air in from the inlet duct and vents hot air out the top of the concrete structure. The condensate inside containment is directed back into the IRWST and the containment sump where it becomes a source of cool water in the sump recirculation process. Early in a LOCA transient, cold water is sprayed by gravity draining onto the containment vessel head to enhance containment cooling. A large tank of water, located at the top of the containment structure, serves as the source of water for this operation.

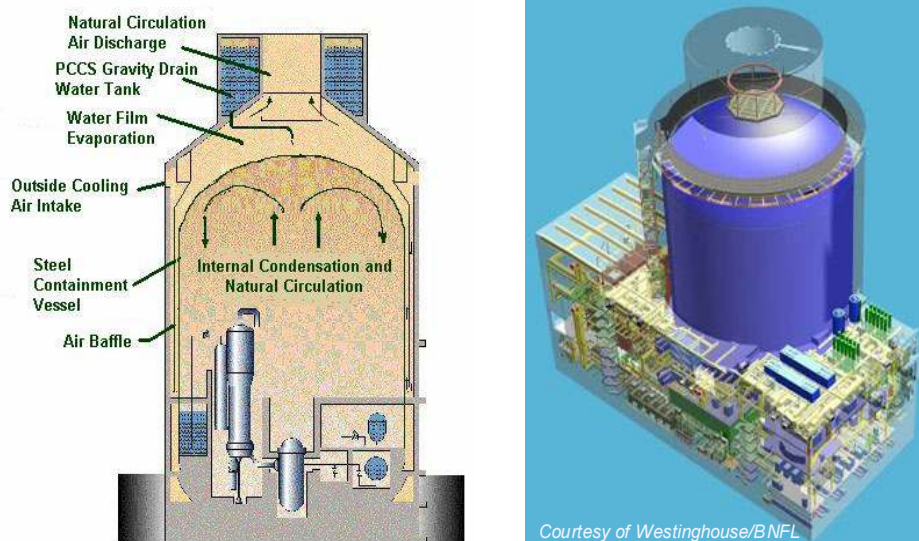


FIG. 6. Containment and passive containment cooling system (PCCS).

2.1.1. Integrated passive safety system response during a SBLOCA

The most effective means of describing the function of each of these passive safety systems is to relate their operation in response to a Small Break Loss-of-Coolant-Accident (SBLOCA). The first phase of a SBLOCA is the subcooled blowdown phase. During this phase, high-pressure subcooled liquid is venting from the break under choked flow conditions. The primary system pressure and primary liquid

inventory will be decreasing. When low pressure or low liquid level is sensed in the pressurizer, a safety signal is issued that results in the following automatic actions:

- Scram reactor,
- Open the PRHR inlet and outlet valves,
- Open the CMT outlet valves,
- Isolate Steam Generators (Feedwater and Main Steam),
- Trip Reactor Coolant Pumps (Coastdown).

Natural circulation is established in the PRHR loop and the CMT loops. Boiling occurs on the PRHR tubes and hot water begins to fill the top of the CMTs. If the plant continues to depressurize, eventually the primary system reaches the saturation pressure corresponding to the hot leg temperature. Depending on the break size, the system pressure will reach a plateau during which the loop will experience a period of two-phase natural circulation.

If primary coolant inventory continues to decrease, eventually the CMTs will begin to drain. At a predetermined CMT level, the ADS-1 valves will open followed by the ADS 2-3 valves. System pressure will drop very quickly as a result of the ADS 1-3 venting steam into the IRWST. The primary system pressure soon drops below the accumulator tank pressure significant quantities of cold borated water are injected into the reactor vessel.

If the CMT liquid level continues to decrease, the ADS-4 actuation setpoint will be reached. The ADS-4 valves open, dropping primary system pressure below the head pressure of the IRWST liquid. The IRWST drains by gravity into the reactor vessel, out the break and ADS 4 valves into the containment sump. Eventually the IRWST and containment sump liquid levels equalize and long term sump recirculation cooling is established by opening the sump valves.

Steam vented through the ADS-4 valves is condensed on the inside surfaces of the containment vessel and the containment vessel is externally cooled by air and water as needed. The condensate inside containment is returned to the containment sump and IRWST where it is available to sump recirculation cooling.

3. PASSIVE SAFETY INJECTION SYSTEMS

This chapter provides some simple models for passive safety injection systems of the type used in the AP600 and AP1000 designs. It includes a description of the governing equations for pressurized and gravity drain tanks. These are applicable to the accumulators, CMTs, and IRWST. Scaling relations are also provided for passive safety injection experiment design.

3.1. Governing equations

Figure 7 shows the simple passive safety system tank considered in this section. The pressure at the liquid free surface is denoted by P_{FS} . The pressure at the injection line exit is denoted by P_E . Most passive safety tanks are filled with cold borated water. Hence, it is reasonable to assume that the working fluid is incompressible. The cross-sectional area of the tank, A_{Tank} , is assumed constant for this analysis. The injection flow area is denoted by A_E . The injection lines usually include multiple check valves, isolation valves and bends. As a result, the form loss coefficient, K , typically dominates the pressure drop in the line.

The injection mass flow rate is denoted by \dot{m}_{inj} and the time dependent liquid level by $L(t)$.

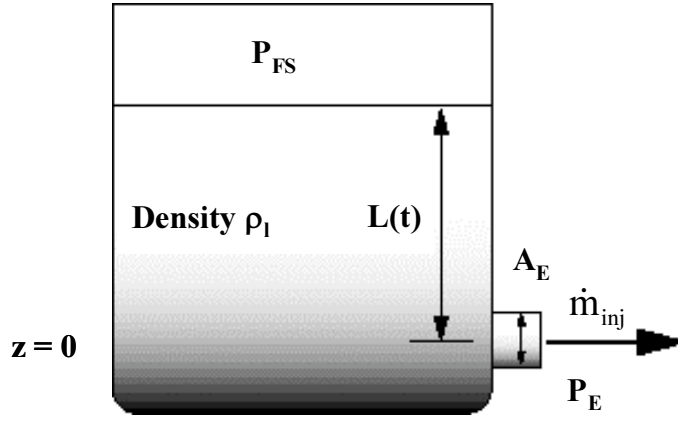


FIG. 7. Schematic for a passive safety system tank.

The governing equations for a passive safety injection tank are provided in Table 1. These equations will be examined for two types of passive safety systems. The first passive safety system implements tanks that drain under the influence of gravity, such as the CMT or the IRWST. The second passive system uses a pressurized tank to inject coolant, such as an accumulator.

Table 1. Governing equations for a passive safety system injection tank

<u>Governing Equations</u>	
<i>Mass Conservation:</i>	
	$\rho_l A_{Tank} \frac{dL}{dt} = -\dot{m}_{inj} \quad (1)$
<i>Bernoulli Equation:</i>	
	$\frac{P_{FS}}{\rho_l g} + z_{FS} + \frac{v_{FS}^2}{2g} = \frac{P_E}{\rho_l g} + z_E + \frac{v_E^2}{2g} + h_l \quad (2)$
<i>Darcy Formula:</i>	
	$h_l = \frac{v_E^2}{2g} \left(\frac{fl}{d} + K \right)_E = \frac{v_E^2}{2g} \Pi_{FE} \quad (3)$
<u>Governing Differential Equation</u>	
	$\rho_l A_{Tank} \frac{dL}{dt} = -\dot{m}_o \left[\frac{\Delta P + \rho_l g L}{\Delta P_o + \rho_l g L_o} \right]^{1/2} \quad (4)$
where:	
	$\dot{m}_o = A_E \left\{ \frac{2\rho_l (\Delta P_o + \rho_l g L_o)}{1 + \Pi_{FE}} \right\}^{1/2} \quad (5)$

3.2. Gravity draining tanks (CMT and IRWST)

For tanks that drain by gravity, it is assumed that the static pressure at the free surface equals that at the injection line exit. Thus the governing differential equation is given by equation (6) in Table 2. Using the initial conditions described by equations (7) and (8), the governing differential equation can be written in dimensionless form as given by equation (9). Equation (11) defines a characteristic residence time, τ , as the ratio of the initial liquid mass in the tank and the initial injection flow rate. Equation (9) can be integrated to obtain a very simple expression for the liquid level as a function of time.

Table 2. Governing equations and analytical solution for a gravity drain tank

<u>Governing Differential Equation</u>	
	$\rho_l A_{Tank} \frac{dL}{dt} = -\rho_l A_E \left\{ \frac{2gL}{1+\Pi_{FE}} \right\}^{1/2} \quad (6)$
<u>Initial Conditions</u>	
	$M_o = \rho_l A_{Tank} L_o \quad (7)$
	$\dot{m}_o = \rho_l A_E \left\{ \frac{2gL_o}{1+\Pi_{FE}} \right\}^{1/2} \quad (8)$
<u>Dimensionless Equation</u>	
	$\frac{dL^+}{dt^+} = -(L^+)^{1/2} \quad (9)$
where	$L^+ = \frac{L}{L_o} \quad (10)$
	$\dot{m}^+ = \frac{\dot{m}}{\dot{m}_o} \quad (11)$
	$t^+ = \frac{t}{\tau} = \frac{t}{(M_o/\dot{m}_o)} \quad (12)$
<u>Analytical Solutions</u>	
	$L^+ = \left(1 - \frac{t^+}{2} \right)^2 \quad (13)$
	$\dot{m}^+ = \left(1 - \frac{t^+}{2} \right) \quad (14)$
Ranges:	$0 \leq L^+ \leq 1$
	$0 \leq t^+ \leq 2$
	$0 \leq \dot{m}^+ \leq 1$

Figure 8 presents a universal curve for gravity draining for the case of a tank with constant cross-sectional area with an incompressible working fluid and an exit line pressure drop that is dominated by form losses.

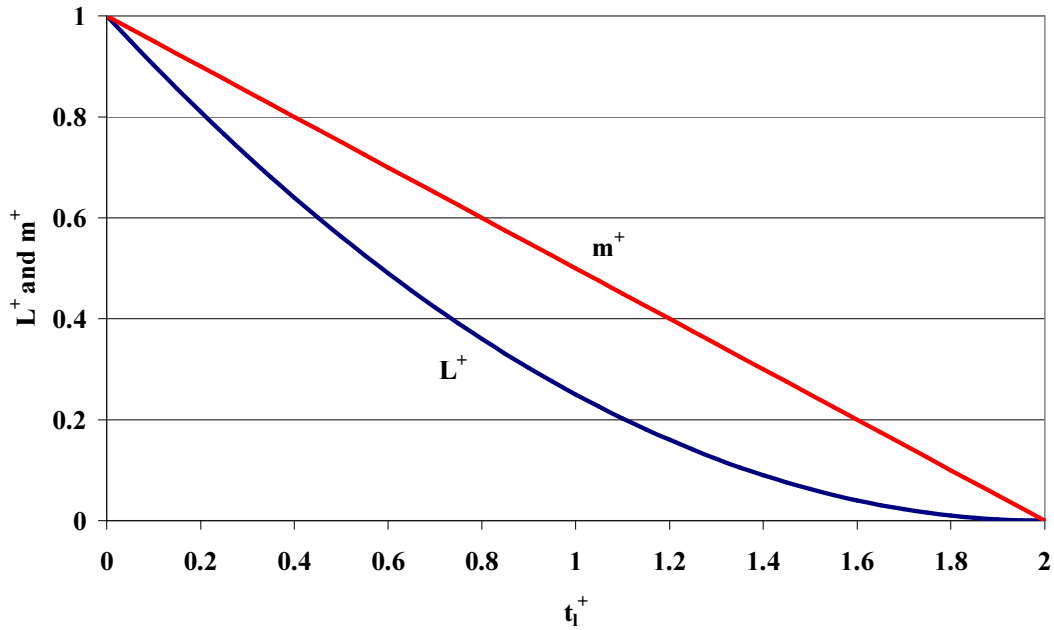


FIG. 8. Gravity draining curve of dimensionless liquid level and injection mass flow rate versus dimensionless time. (Constant tank cross-sectional area, incompressible fluid, form loss dominated at exit).

Table 3 illustrates how one can use the dimensionless groups presented above to develop similarity criteria for the design of a passive safety system experiment. It is important to note that the designer has many choices in the process. For example, the tank length scale ratio and cross-sectional area ratio can be selected based on commercial availability and cost. However, if the tank is connected to an integral system, such flexibility might be lost because other factors may be fixed, such as the injection mass flow rate scale ratio. Using the same working fluid usually simplifies the problem. The example provided is illustrative of the process.

Table 3. Similarity criteria for the design of a passive safety system gravity drain tank

<u>Similarity Criteria</u>	
$L_R^+ = \frac{\left(\frac{L}{L_o}\right)_m}{\left(\frac{L}{L_o}\right)_p} = 1 \quad (15)$	$t_R^+ = \frac{\left(\frac{t}{\tau}\right)_m}{\left(\frac{t}{\tau}\right)_p} = 1 \quad (16)$
<u>Scaling Example</u>	
<p><i>Scale Model Requirements</i></p> <ul style="list-style-type: none"> • Time Scale Ratio = 1:2 • Length Scale Ratio = 1:4 • Tank Area Ratio = 1:50 • Fluid Property Similitude (i.e., same working fluid) 	
<p><i>Scale Ratios</i></p> $t_R = \tau_R = \frac{(M_o)_R}{(\dot{m}_o)_R} = \frac{1}{2} \quad (17)$ <p>Hence:</p> $(M_o)_R = (A_{Tank})_R (L_o)_R = \frac{1}{200} \quad (18)$ <p>Substituting into (15) yields:</p> $(\dot{m}_o)_R = \frac{1}{100} \quad (19)$ <p>Preserving the $\frac{1}{2}$ time scale in a $\frac{1}{4}$ length scale injection line requires the fluid to travel at a $\frac{1}{2}$ velocity ($L_R/t_R = \frac{1}{2}$). This yields the design requirement:</p> $(A_E)_R = \frac{1}{50} \quad (20)$ <p>Lastly, equation (8) is used to obtain the following, scale ratio:</p> $(\dot{m}_o)_R = \frac{(A_E)_R (L_o)_R^{\frac{1}{2}}}{(\Pi_{FE})_R^{\frac{1}{2}}} = \frac{(A_E)_R}{2(\Pi_{FE})_R^{\frac{1}{2}}} \quad (21)$ <p>Substituting the length scale ratio and the injection line flow area ratio yields the last design requirement needed to</p> $(\Pi_{FE})_R = 1 \quad (22)$	

3.3. Pressurized coolant injection tanks (accumulators)

This section presents an analysis for the liquid discharge of a pressurized tank into a reservoir having a fixed backpressure. In actual practice, the backpressure would be decreasing at a rate dictated by the overall system transient.

For pressurized coolant injection tanks, the difference between the charging pressure in the tank and the system pressure is typically much greater than the gravity head of the liquid in the tank. Hence the gravity term can be neglected. It has been assumed that the liquid is incompressible. Because the tanks are normally quite large, the expansion of the gas can be relatively slow, particularly during a SBLOCA. Thus, the assumption that the gas expands isothermally is reasonable. However, this assumption becomes less applicable to the LBLOCA. Therefore a second analysis was conducted assuming an isentropic expansion of the gas. The similarity criteria will remain the same for both bases. Table 4 lists the governing equations for the pressurized injection tank.

Table 4. Governing equations for a passive safety system pressurized injection tank

<u>Governing Equations</u>	
<i>Mass Conservation (Liquid):</i>	
	$\rho_l \frac{dV_l}{dt} = -\dot{m}_o \left(\frac{P - P_E}{P_o - P_E} \right)^{1/2} \quad (23)$
<i>Bernoulli Equation (Liquid):</i>	
	$\frac{P}{\rho_l g} + z_{FS} + \frac{v_{FS}^2}{2g} = \frac{P_E}{\rho_l g} + z_E + \frac{v_E^2}{2g} + h_l \quad (24)$
<i>Darcy Formula (Liquid Injection Line):</i>	
	$h_l = \frac{v_E^2}{2g} \left(\frac{fl}{d} + K \right)_E = \frac{v_E^2}{2g} \Pi_{FE} \quad (25)$
<i>Component Volumes:</i>	
	$V_g = V_{Tank} - V_l \quad (26)$
<i>Isothermal Expansion (Gas):</i>	
	$P_o V_{go} = P V_g \quad (27)$
<i>Isentropic Expansion (Gas):</i>	
	$\frac{P}{P_o} = \left(\frac{V_{go}}{V_g} \right)^{\gamma} \quad (28)$

Table 5 presents the depressurization rate equations for the case of isothermal expansion and isentropic expansion of the charging gas. The governing differential equations are very similar. The solution to the isentropic case is an approximate integral, nonetheless the two results are similar as shown in Figures 9 and 10.

Table 5. Governing differential equation and analytical solutions

<p>Dimensionless Terms:</p> $P^+ = \frac{P}{P_o}$ $P_E^+ = \frac{P_E}{P_o}$ $\Delta P_E^+ = 1 - P_E^+$ $\Delta P^+ = P^+ - P_E^+$ $t_g^+ = \frac{t}{\tau_g} = \frac{t}{(\rho_l V_{go} / \dot{m}_o)}$	
<p>Isothermal Expansion:</p> $\frac{dP^+}{dt^+} = -(P^+)^2 \left[\frac{\Delta P^+}{\Delta P_E^+} \right]^{1/2} \quad (29)$ <p>Analytical Solution: (31)</p> $\frac{(\Delta P^+)^{1/2}}{P^+} + \frac{1}{(P_E^+)^{1/2}} \tan^{-1} \left(\frac{\Delta P^+}{P_E^+} \right)^{1/2} = \phi - \frac{P_E^+ t_g^+}{(\Delta P_E^+)^{1/2}}$ <p>where:</p> $\phi = (\Delta P_E^+)^{1/2} + \frac{1}{(P_E^+)^{1/2}} \tan^{-1} \left(\frac{\Delta P_E^+}{P_E^+} \right)^{1/2}$	<p>Isentropic Expansion:</p> $\frac{dP^+}{dt^+} = -\gamma (P^+)^{\gamma+1} \left[\frac{\Delta P^+}{\Delta P_E^+} \right]^{1/2} \quad (32)$ <p>Analytical Solution: (33)</p> $P^+ \approx \frac{4P_E^+ \Delta P_E^+}{4\Delta P_E^+ - (2\Delta P_E^+ - \gamma P_E^+ t_g^+)^2}$

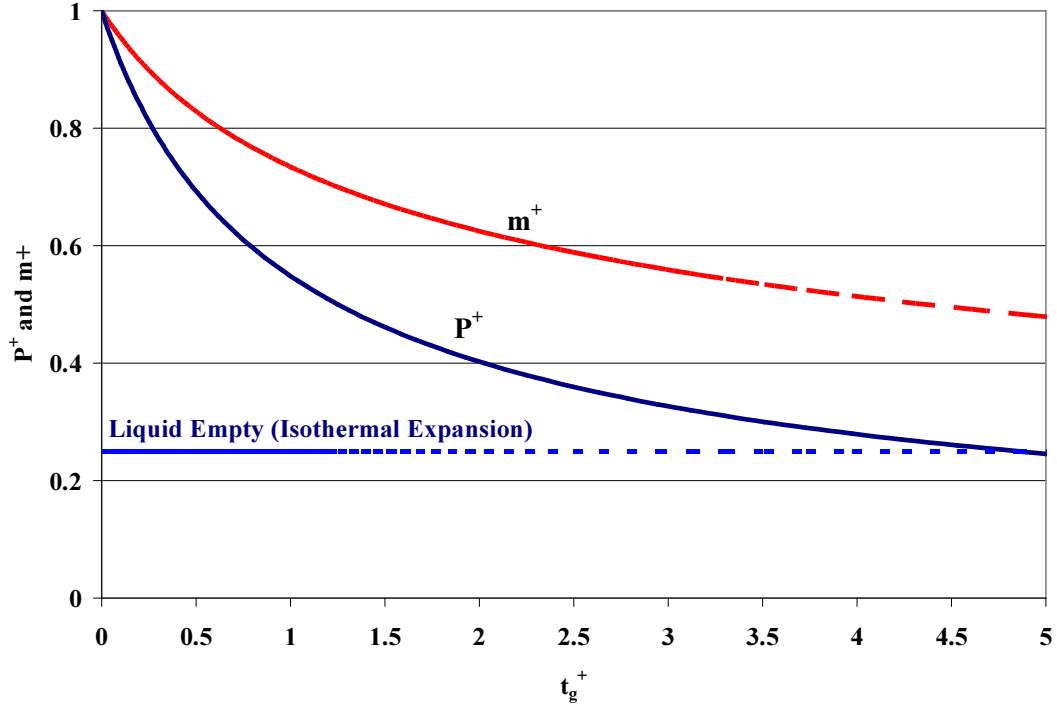


FIG. 9. Accumulator depressurization and liquid injection versus time in dimensionless coordinates (isothermal gas expansion).

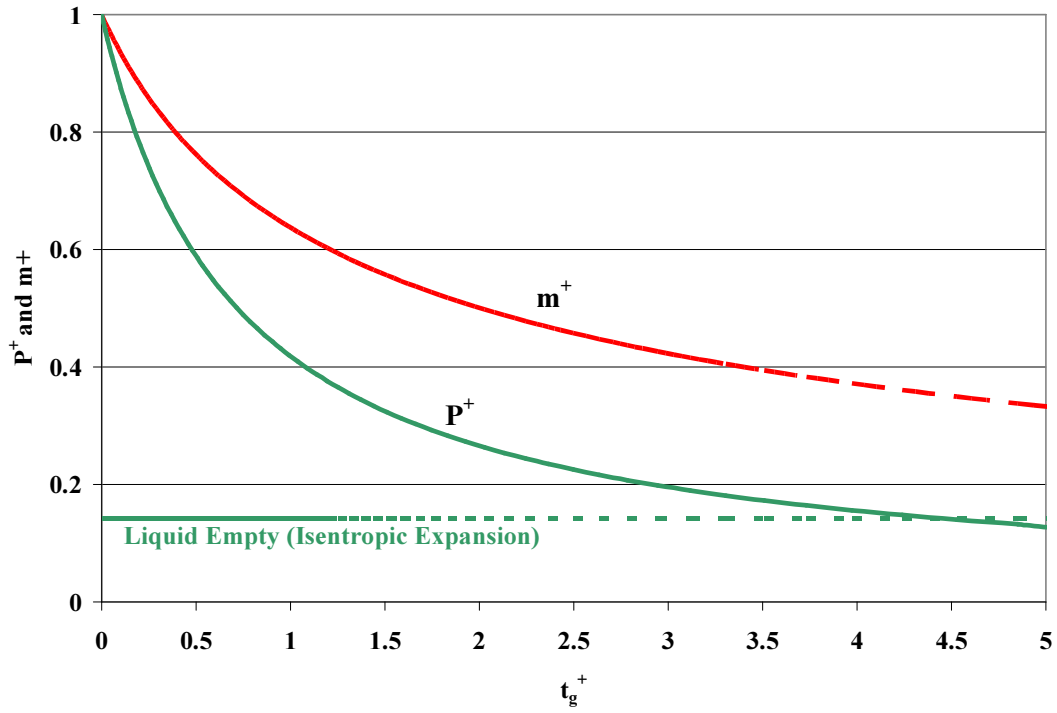


FIG. 10. Accumulator depressurization and liquid injection versus time in dimensionless coordinates (isentropic gas expansion).

4. AUTOMATIC DEPRESSURIZATION SYSTEMS (ADS)

The AP600 and AP1000 implements an Automatic Depressurization System to reduce primary side pressure to containment pressure in a controlled manner. This section presents a Reactor Coolant System (RCS) depressurization rate equation and similarity criteria for the ADS valve flow areas.

4.1. Governing equations for RCS two-phase fluid depressurization

The mass conservation equation for a RCS control volume undergoing a depressurization event is given by:

$$\frac{dM}{dt} = \sum \dot{m}_{inj} - \sum \dot{m}_{ADS} \quad (34)$$

where M is the fluid mass within the RCS and \dot{m} represents the mass flow rate entering or leaving the reactor coolant system. The energy conservation equation for the RCS fluid is expressed as follows:

$$\frac{dU}{dt} = \sum (\dot{m}h)_{inj} - \sum (\dot{m}h)_{ADS} + \dot{q}_{SG} + \dot{q}_{core} + \dot{q}_{loss} - P \frac{dV}{dt} \quad (35)$$

where U is the bulk internal energy of the fluid within the RCS, h is the enthalpy of the fluid entering or leaving the RCS, \dot{q}_{SG} , \dot{q}_{core} and \dot{q}_{loss} are the steam generator energy transfer rate, the core power and the heat loss respectively. P is the RCS pressure and V is the RCS volume. The specific internal energy and the specific volume are defined respectively as follows:

$$e = \frac{U}{M} \quad (36)$$

$$v = \frac{V}{M} \quad (37)$$

The total change in specific internal energy is written in terms of partial differentials with respect to pressure and specific volume as follows:

$$de = \left(\frac{\partial e}{\partial p} \right)_v dp + \left(\frac{\partial e}{\partial v} \right)_p dv \quad (38)$$

Substituting equation (39) into (38) yields:

$$\frac{dMe}{dt} = \sum (\dot{m}h)_{inj} - \sum (\dot{m}h)_{ADS} + \dot{q}_{SG} + \dot{q}_{core} + \dot{q}_{loss} - P \frac{dV}{dt} \quad (39)$$

Expanding the term on the LHS of equation (39), substituting equation (34) and rearranging yields:

$$M \frac{de}{dt} = (\sum \dot{m}_{inj}) (h_{inj} - e) - (\sum \dot{m}_{ADS}) (h_{ADS} - e) + \dot{q}_{SG} + \dot{q}_{core} + \dot{q}_{loss} - P \frac{dV}{dt} \quad (40)$$

In equation (40), it has been assumed that h_{in} is the same for all the injection locations and h_{out} is the same for all the vent paths. Substituting equation (38) into (40), and rearranging yields

$$\begin{aligned} M \left(\frac{\partial e}{\partial P} \right)_v \frac{dP}{dt} &= (\sum \dot{m}_{inj}) (h_{inj} - e) - (\sum \dot{m}_{ADS}) (h_{ADS} - e) \\ &+ \dot{q}_{SG} + \dot{q}_{core} + \dot{q}_{loss} - P \frac{dV}{dt} - M \left(\frac{\partial e}{\partial v} \right)_p \frac{dv}{dt} \end{aligned} \quad (41)$$

Using equation (37), and the mass conservation equation, the last term on the RHS of equation (41) is written as:

$$M \left(\frac{\partial e}{\partial v} \right)_p \frac{dv}{dt} = \left(\frac{\partial e}{\partial v} \right)_p \frac{dV}{dt} - v \left(\frac{\partial e}{\partial v} \right)_p (\sum \dot{m}_{inj} - \sum \dot{m}_{ADS}) \quad (42)$$

Substituting back into equation (41) yields:

$$\begin{aligned} M \left(\frac{\partial e}{\partial P} \right)_v \frac{dP}{dt} &= (\sum \dot{m}_{inj}) \left[h_{inj} - e + v \left(\frac{\partial e}{\partial v} \right)_p \right] \\ &- (\sum \dot{m}_{ADS}) \left[h_{ADS} - e + v \left(\frac{\partial e}{\partial v} \right)_p \right] \\ &+ \dot{q}_{SG} + \dot{q}_{core} + \dot{q}_{loss} - \left[P + \left(\frac{\partial e}{\partial v} \right)_p \right] \frac{dV}{dt} \end{aligned} \quad (43)$$

which is the “depressurization rate equation.” For the RCS control volume, which has rigid boundaries, equation (43) becomes:

$$\begin{aligned} M \left(\frac{\partial e}{\partial P} \right)_v \frac{dP}{dt} &= (\sum \dot{m}_{inj}) \left[h_{inj} - e + v \left(\frac{\partial e}{\partial v} \right)_p \right] \\ &- (\sum \dot{m}_{ADS}) \left[h_{brk} - e + v \left(\frac{\partial e}{\partial v} \right)_p \right] + \dot{q}_{SG} + \dot{q}_{core} + \dot{q}_{loss} \end{aligned} \quad (44)$$

The net energy transfer rate is given as:

$$\dot{q}_{net} = \dot{q}_{SG} + \dot{q}_{core} + \dot{q}_{loss} \quad (45)$$

Equation (44) is the governing equation for depressurization behavior in the RCS. Table 6 summarizes the governing equations and normalizing ratios for RCS depressurization. Table 7 presents the

dimensionless balance equations and the dimensionless groups that should be preserved in a scaled test facility [4],[5].

Table 6. Governing equations and normalizing ratios for RCS depressurization

<p><u>Governing Balance Equations</u></p> <p><i>Mass Balance Equation:</i></p> $\frac{dM}{dt} = \sum \dot{m}_{inj} - \sum \dot{m}_{ADS} \quad (46)$ <p><i>Depressurization Rate Equation:</i></p> $M \left(\frac{\partial e}{\partial P} \right)_v \frac{dP}{dt} = (\sum \dot{m}_{inj}) \left[h_{inj} - e + v \left(\frac{\partial e}{\partial v} \right)_p \right] - (\sum \dot{m}_{ADS}) \left[h_{ADS} - e + v \left(\frac{\partial e}{\partial v} \right)_p \right] + \dot{q}_{SG} + \dot{q}_{core} + \dot{q}_{loss} \quad (47)$	
<p><u>Normalized Initial and Boundary Conditions</u></p> $t^+ = \frac{t}{\tau_{RCS}} \quad (48)$ $M^+ = \frac{M}{M_o} \quad (49)$ $P^+ = \frac{P}{P_o} \quad (50)$ $\dot{q}_{net}^+ = \frac{\dot{q}_{net}}{\dot{q}_{net,o}} \quad (51)$ $\sum \dot{m}_{inj}^+ = \frac{\sum \dot{m}_{inj}}{\sum \dot{m}_{inj,o}} \quad (52)$	$\sum \dot{m}_{ADS}^+ = \frac{\sum \dot{m}_{ADS}}{\sum \dot{m}_{ADS,o}} \quad (53)$ $\left[h_{inj} - e + v \left(\frac{\partial e}{\partial v} \right)_p \right]^+ = \frac{\left[h_{inj} - e + v \left(\frac{\partial e}{\partial v} \right)_p \right]}{\left[h_{inj} - e + v \left(\frac{\partial e}{\partial v} \right)_p \right]_o} \quad (54)$ $\left[h_{ADS} - e + v \left(\frac{\partial e}{\partial v} \right)_p \right]^+ = \frac{\left[h_{ADS} - e + v \left(\frac{\partial e}{\partial v} \right)_p \right]}{\left[h_{ADS} - e + v \left(\frac{\partial e}{\partial v} \right)_p \right]_o} \quad (55)$

Table 7. Dimensionless equations and Π groups for RCS depressurization

<p><u>Dimensionless Balance Equations</u></p> <p><i>RCS Mass Balance Equation:</i></p> $\tau_{RCS} \frac{dM^+}{dt} = \Pi_m \Sigma \dot{m}_{inj}^+ - \Sigma \dot{m}_{ADS}^+ \quad (56)$ <p><i>RCS Depressurization Rate Equation:</i></p> $M^+ \left(\frac{\partial e}{\partial P} \right)_v^+ \tau_{RCS} \frac{dP^+}{dt} = \frac{\Pi_h}{\Pi_\varepsilon} \Sigma \dot{m}_{inj}^+ \left[h_{inj} - e + v \left(\frac{\partial e}{\partial v} \right)_p \right]^+ - \frac{\Sigma \dot{m}_{ADS}^+}{\Pi_\varepsilon} \left[h_{ADS} - e + v \left(\frac{\partial e}{\partial v} \right)_p \right]^+ + \frac{\Pi_\Gamma}{\Pi_\varepsilon} q_{net}^+ \quad (57)$	
<p><u>Characteristic Time Constant</u></p> $\tau_{res} = \frac{M_o}{\Sigma \dot{m}_{ADS,o}} \quad (58)$	
<p><u>Dimensionless Groups</u></p> <p><i>Mass Balance Number:</i></p> $\Pi_m = \frac{\Sigma \dot{m}_{inj,o}}{\Sigma \dot{m}_{ADS,o}} \quad (59)$ <p><i>Enthalpy Balance Number:</i></p> $\Pi_h = \frac{\Sigma \dot{m}_{inj,o} \cdot \left[h_{inj} - e + v \left(\frac{\partial e}{\partial v} \right)_p \right]_o}{\Sigma \dot{m}_{ADS,o} \cdot \left[h_{Brk} - e + v \left(\frac{\partial e}{\partial v} \right)_p \right]_o} \quad (60)$	<p><i>Heat Source Number:</i></p> $\Pi_\Gamma = \frac{\dot{q}_{net,o}}{\Sigma \dot{m}_{ADS} \cdot \left[h_{brk} - e + v \left(\frac{\partial e}{\partial v} \right)_p \right]_o} \quad (61)$ <p><i>Fluid Mixture Dilation Number:</i></p> $\Pi_\varepsilon = \varepsilon_o = \frac{P_o \left(\frac{\partial e}{\partial P} \right)_{v,o}}{\left[h_{ADS} - e + v \left(\frac{\partial e}{\partial v} \right)_p \right]_o} \quad (62)$

The dimensionless group, Π_h , is the energy flow rate ratio. It represents the ratio of the total energy change due to fluid injection to the energy change caused by the break flow. Π_r is the power ratio. It represents the ratio of the net heat into the system to the rate of fluid energy transport through the break. Π_e is the fluid mixture dilation property group. Equation (62) reveals that the fluid dilation property group couples the system intensive energy change to the intensive energy at the break. For high pressure systems venting to the ambient, the fluid properties at the break are determined at critical flow conditions. Evaluating the RCS time constant, τ_{RCS} , and the dimensionless groups Π_m , Π_h , Π_r , Π_e requires knowledge of the pressure dependent fluid properties and the critical mass flux.

For the case of fluid property similitude, all of the dimensionless groups simplify to produce the simple set of scale ratios presented in Table 8. For fluid property similitude, the critical mass flux in the model, $(G_{ADS})_m$, would be identical to that in the prototype and the ratio of Π_e would be unity.

Table 8. RCS depressurization scale ratios assuming for isochronicity and fluid property similitude

Fluid Property Similitude Yields:

$$\begin{aligned} (G_{ADS,o})_R &= 1 \\ (M_o)_R &= (V_o)_R \\ (\dot{m}_{ADS,o})_R &= (A_{ADS,o})_R \end{aligned}$$

Scale Ratios

$$(\tau_{RCS})_R = \left(\frac{M_o}{\dot{m}_{ADS,o}} \right)_R = \left(\frac{V_o}{A_{ADS,o}} \right)_R = 1 \quad (63)$$

Flow Area Scaled to Volume :

$$(A_{ADS})_R = (V_o)_R \quad (64)$$

Injection Flow Rates Scaled to Volume:

$$(\dot{m}_{inj,o})_R = (A_{ADS})_R = (V_o)_R \quad (65)$$

Power Scaled to Volume:

$$(\dot{q}_{net,o})_R = (A_{ADS})_R = (V_o)_R \quad (66)$$

5. COMPARISON OF APEX-600 AND SPES PASSIVE SAFETY SYSTEM RESPONSES

The AP600 design has undergone extensive testing for plant certification. Three scaled integral system test facilities were operated to assess passive safety system performance; ROSA-AP600, SPES-2 and APEX-600. This section presents a brief comparison of a two-inch break simulation conducted in the Full Height-Full Pressure SPES-2 and in the Quarter Height Reduced Pressure OSU APEX. Table 9 presents the scale ratios for each of the facilities.

Table 9. Scale ratios for SPES-2 and APEX-600 relative to AP600

Scaling Ratios	APEX	SPES-2
Lengths	1:4	1:1
Relative elevations	1:4	1:1
Flow Areas	1:48	1:395
Volumes	1:192	1:395
Decay Power	1:96	1:395
Fluid Velocity	1:2	1:1
Fluid Transient Time	1:2	1:1
Mass Flow Rate	1:96	1:395

Figure 11 outlines a typical SBLOCA scenario. Initially there is a sharp decrease in system pressure due to the subcooled blowdown of fluid from the break. Being a reduced pressure test facility, the APEX-600 test facility did not model this portion of the transient. It begins the simulation when the system has reached saturated conditions. Subsequent to that point, all of the safety system actions were simulated by both facilities. Figures 12 through 16 compare the dimensionless depressurization histories, the CMT draining and flow behavior, and the Accumulator draining and flow behavior. The plots show excellent agreement between the two facilities and support the scaling methods used to design the facilities.

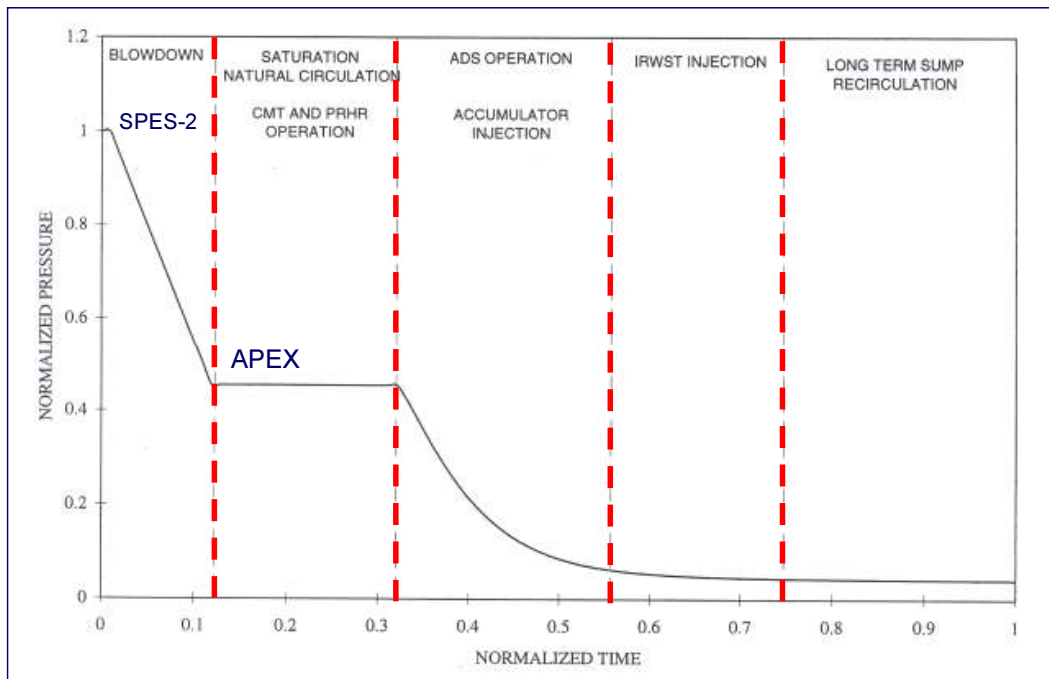


FIG. 11. Typical phases of an AP600/AP1000 SBLOCA pressure history.

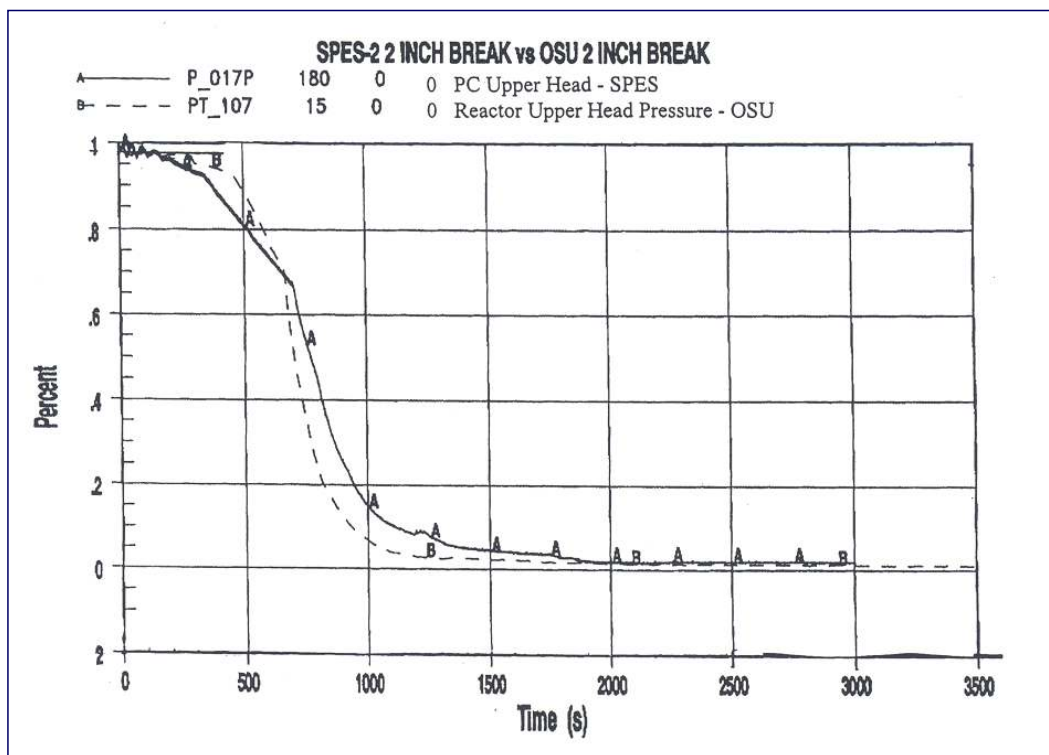


FIG. 12. Comparison of SPES-2 and APEX-600 two-inch SBLOCA pressure histories.

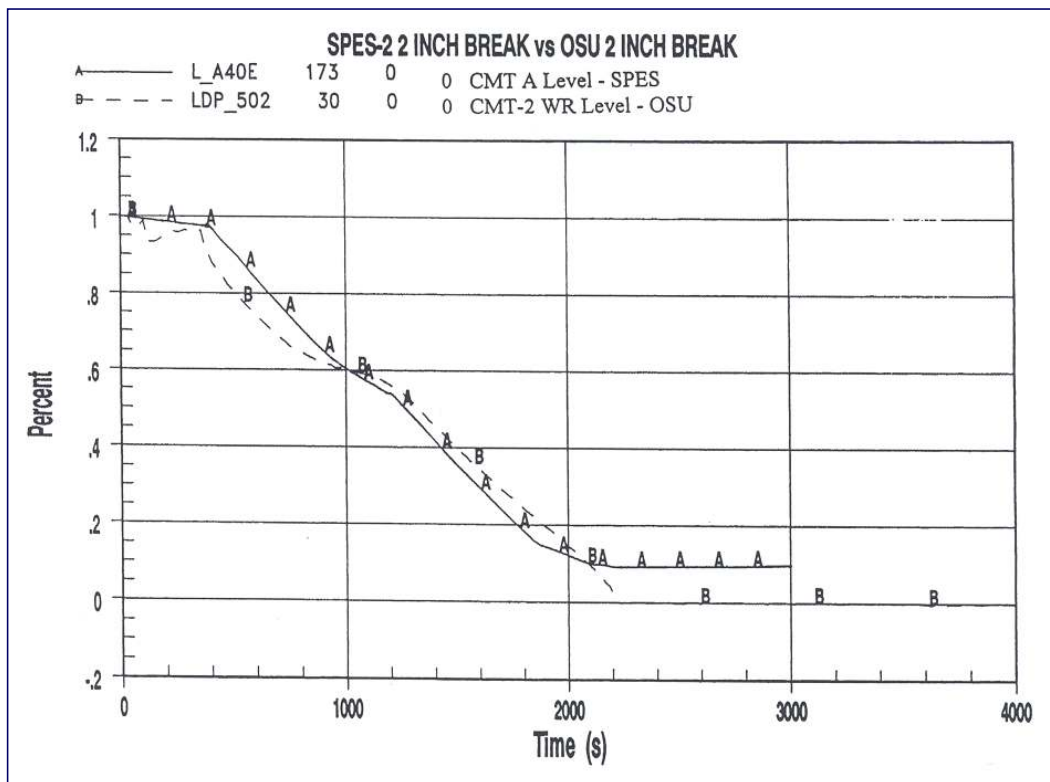


FIG. 13. Comparison of SPES-2 and APEX-600 two-inch SBLOCA CMT level histories.

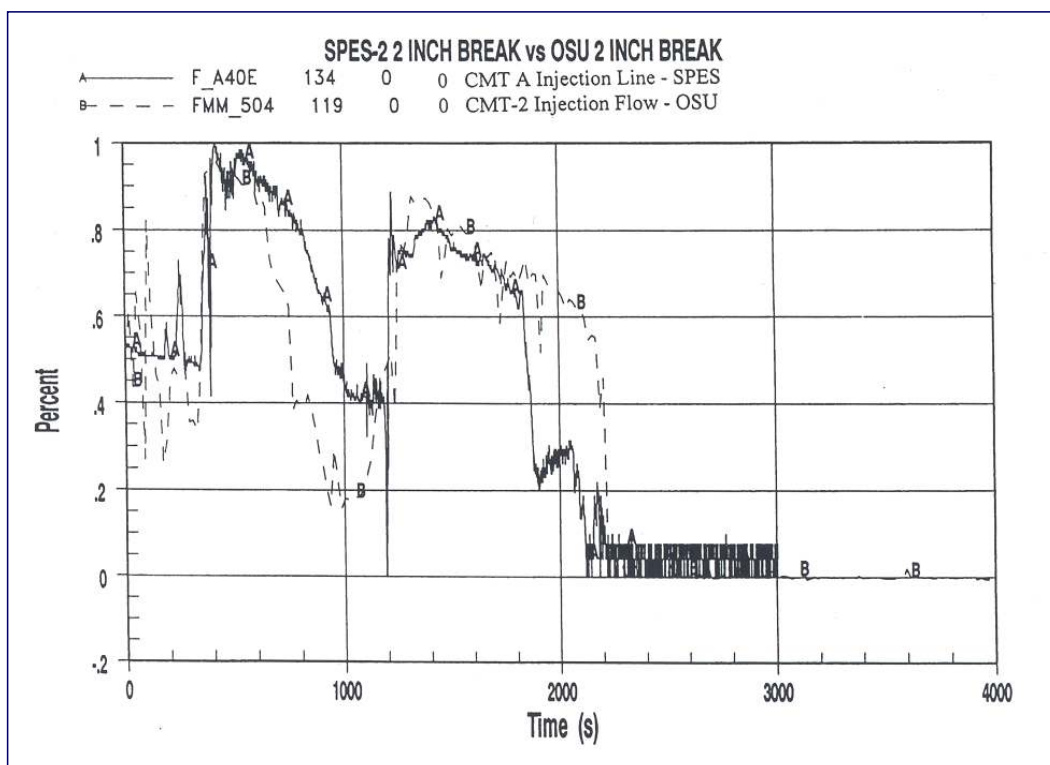


FIG. 14. Comparison of SPES-2 and APEX-600 two-inch SBLOCA CMT flow histories.

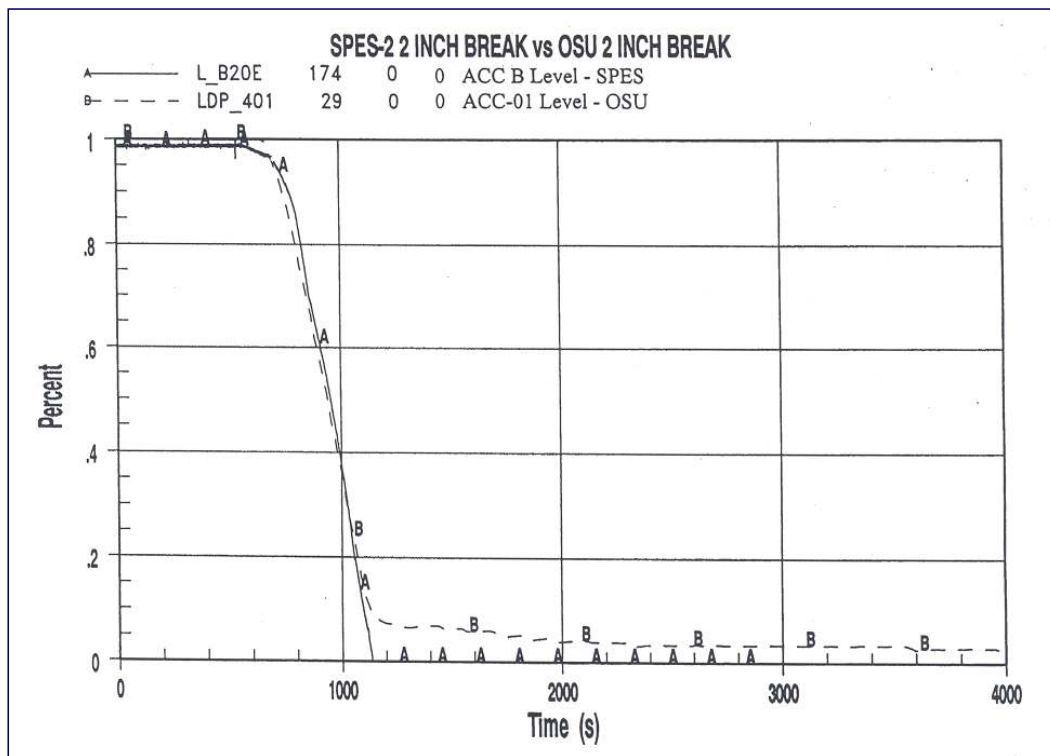


FIG. 15. Comparison of SPES-2 and APEX-600 two-inch SBLOCA accumulator liquid level histories.

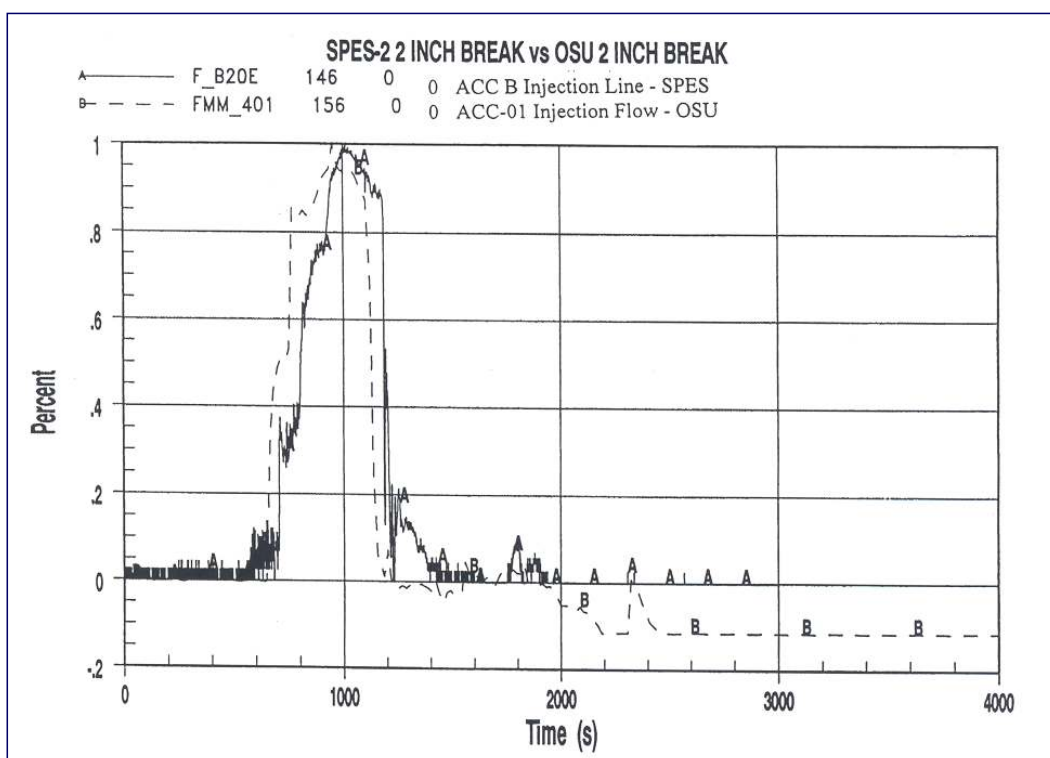


FIG. 16. Comparison of SPES-2 and APEX-600 two-inch accumulator flow histories.

NOMENCLATURE

Acronyms

ACC	Accumulator Tank
ADS	Automatic Depressurization System
CMT	Core Make-up Tanks
CS	Containment Sump
IRWST	In-containment Refueling Water Storage Tank
PCCS	Passive Containment Cooling System
PRHR	Passive Residual Heat Removal System

Symbols

A	cross-sectional area
d	line diameter
e	specific internal energy
f	friction factor
g	gravitational constant
G	mass flux
h_l	head loss
h_{inj}	enthalpy of injected liquid
h_{ADS}	enthalpy of ADS vapor
K	loss coefficient
l	line length
L	level
\dot{m}	mass flow rate
M	Mass
P	static pressure
\dot{q}	heat loss or power
t	time
v_E	liquid velocity at exit
v	specific volume
V	volume
Z	elevation

Greek Symbols

γ	ratio of specific heats
$\Pi_{FE} = \left(\frac{fl}{d} + K \right)_E$	
ρ	density

ACKNOWLEDGEMENT

This work was supported through a U.S. Department of Energy Contract (DE- FC07-04ID14550) and the Oregon State University sabbatical program. This work was conducted through the IAEA Nuclear Power Technology Development Section.

REFERENCES

- [1] INTERNATIONAL ATOMIC ENERGY AGENCY, Safety related terms for advanced nuclear plants, IAEA-TECDOC-626, September 1991.
- [2] Title 10, Energy, Code of Federal Regulations, Part 50, Office of Federal Register, National Archives and Records Administration, Available through Superintendent of Documents, U.S. Government Printing Office, Washington, D.C. 20402 (2004).
- [3] VERTES, C.M., Passive safeguards design optimization studies for the Westinghouse AP600, Fifth Proceedings of the Nuclear Thermal Hydraulics, 1989 Winter Meeting of the ANS, San Francisco, California, November 26-30 (1989).
- [4] REYES, J.N., JR., RUSHER, C., Analytical models for pressure vessel blowdowns of saturated fluid mixtures, Proceeding of the 1999 NURETH-9 Conference, October 3-8, 1999, San Francisco, CA.
- [5] REYES, J.N., JR., Scaling the depressurization behavior of fluids in phase equilibria, Proceedings of the Japan-U.S. Seminar on Two Phase Flow Dynamics, Kyushu University, Fukuoka, Japan, July 15-20 (1996).